9^{th} ANKARA INTERNATIONAL AEROSPACE CONFERENCE **AIAC-2017-097**
20-22 September 2017 - METU, Ankara TURKEY

VORTEX CLUSTERS IN TURBULENT BOUNDARY LAYER FLOWS SUBJECTED TO ADVERSE PRESSURE GRADIENT

Egemen Aydin* and Ayse G. Gungor†
Faculty of Aeronautics and Astronautics, Istanbul Technical University, 34469 Maslak, Istanbul, Turkey

ABSTRACT

The main objective of this study is to contribute to the understanding of coherent structures by looking at vortex clusters in turbulent boundary layers subject to strong adverse pressure gradient (APG) that encountered on the suction side of a LPT blade. Statistical properties of three-dimensional vortex clusters' dimensions are determined and analyzed. Results show that near wall clusters have more elongation on flow direction while clusters that located away from the wall resemble cubic boxes. Furthermore, our study show that statistical characteristics of vortex clusters do not change with the use of different vortex identification techniques.

INTRODUCTION

Understanding the wall bounded turbulent flows is crucial in improving the energy efficiency of broad engineering systems. Adverse pressure gradient (APG) boundary layer is an extensive part of wall bounded turbulent flows. APG flows are commonly confronted in many engineering applications including fans, turbines, pumps, jet engines, aircrafts, cars and turbo-machinery. APG is the most influential factor in determining efficiency of such devices. By the reason of this occurrence, understanding the behavior of APG flows have great practical importance.

Organized structures in turbulent flows have great importance to understand APG effect and expand our knowledge on turbulent boundary layer flows; since, these coherent structures play essential role in the production and dissipation of wall turbulence [Aubry et al, 1988]. Considerable statistical information of turbulent flows has been acquired by using these coherent structures. Although coherent structures have not any universally accepted specific definition yet, [Hussain, 1983] explains as *"A coherent structure is a connected turbulent fluid mass with instantaneously phase-correlated vorticity over its spatial extent."*.

Vortex clusters, on the other hand, is a special kind of coherent structure [Del Álamo et al, 2006]. Unlike common coherent structure iso-surface visualization, vortex clusters show real appearance. Also each vortex cluster represents single distinct structure. Therefore, vortex clusters are suitable tool to investigate turbulent flows.

There are large number of experimental and numerical studies on the dynamics of coherent structures

*Undergraduate Student in Aero. and Astro. Eng., Email: aydineg@itu.edu.tr
†Assist. Prof. in Faculty of Aeronautics and Astronautics, Email: ayse.gungor@itu.edu.tr

in wall-bounded canonical flows. However, the information on coherent structures found in APG boundary layers is limited in comparison to canonical wall flows. Hence, the purpose of this study is to contribute to the statistical understanding of coherent structures in APG flows.

NUMERICAL METHOD

Since direct numerical simulation (DNS) presents the most detailed interpretation of a turbulent flow field as far as computational methods are concerned, the DNS of [Gungor et al, 2014] is used to study vortex clusters in APG boundary layer flows. In the DNS setup, the flow of interest is formed on a flat plate boundary layer subject to a strong adverse pressure gradient similar to environment of the suction side of T106C high-lift low-pressure-turbine blade. The desired pressure gradient is controlled by imposing a positive uniform wall-normal velocity distribution at the upper boundary of the computational domain. The transition to turbulence scenario is triggered by positioning a two dimensional disturbance strip very close to the inflow.

The simulation parameters are summarized in table 1. L_x, L_y, and L_z are the domain dimensions along the cartesian axes, N_x, N_y, and N_z are the corresponding grid points, and $\Delta x^+, \Delta y^+_{min}, \Delta z^+$ are the resolutions in wall unit. Re_θ is the Reynolds number based on momentum thickness and free-stream velocity, and β is the pressure gradient parameter. A further information can be found in [Gungor et al, 2014].

Table 1: Details of the DNS data.

$(L_x \times L_y \times L_z)/\theta_0$	$N_x \times N_y \times N_z$	$\Delta x^+, \Delta y^+_{min}, \Delta z^+$	Re_θ	β
$2380 \times 450 \times 1100$	$1537 \times 201 \times 768$	$2.2 \times 0.2 \times 2.0$	$\approx 150 - 2200$	5-100

Figure 1 shows the spatial development of the vortical structures. The flow is initially laminar which then separates and transitions within the separation bubble, finally turbulent flow develops under strong adverse pressure gradient. As a major implication of transition, hairpin vortices are observed as shown in the left box. Downstream, hairpin vortices lose their dominance until completion of transition, then densely populated quasi-streamwise vortices emerge in the flow field. Due to presence of APG, population density of these vortices decrease substantially.

Figure 2 presents the turbulent kinetic energy distribution. The time-averaged separation line is also indicated in the figure with white solid line. The growth of turbulence around the reattachment region is apparent. The intensity of the turbulent kinetic energy decreases downstream while the peak location moves away from the wall from the reattachment point to the end of the simulation domain as a result of APG.

Instead of calculating vortex clusters in the whole simulation, the extracted sub-domain was used for the vortex calculation. Along with this extracted domain selection, relatively small effect of separated region on vortex clusters has achieved [Gungor et al, 2014] and the calculation time of clusters has decreased. The dimension of the domain of interest along the three axes are $L_x \times L_y \times L_z \approx 4.51\delta_a \times 2.02\delta_a \times 8.36\delta_a$. Here δ_a is the average boundary layer thickness of the selected domain. Reynolds number, Re_θ, ranges between 1200 and 1967, and shape factor, H, varies between 1.69 and 2.49 along the extraction box.

500 instantaneous DNS fields are processed to extract vortex clusters. As a result of this process approximately two and half million vortex clusters are obtained.

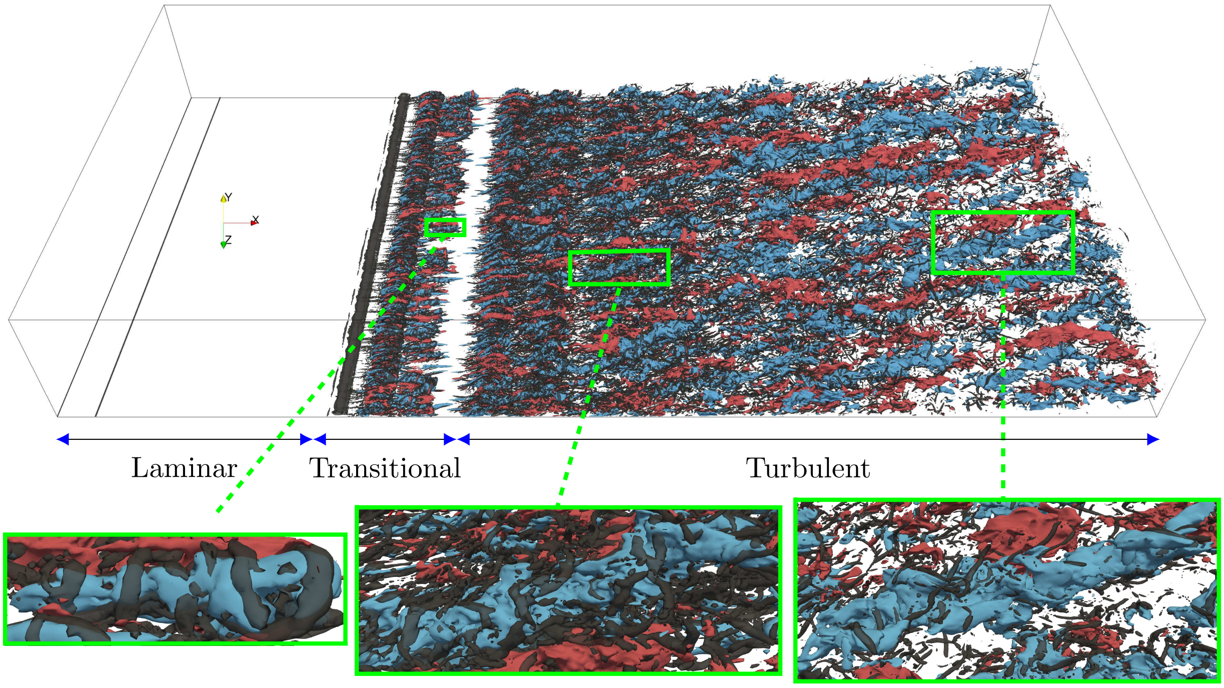

Figure 1: Computational domain, black represents iso-surfaces of the second invariant of the velocity gradient tensor, red represents high speed streaks iso-surfaces of $u' = 0.8$, blue represents low speed streaks iso-surfaces of $u' = -0.8$. Flow direction is from left to right.

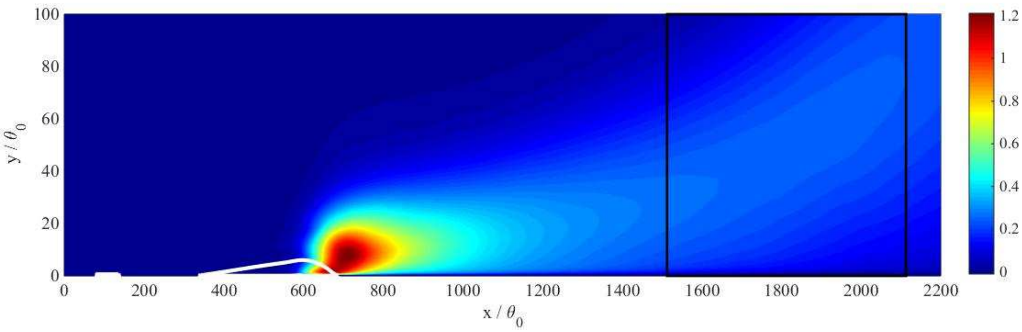

Figure 2: Turbulent kinetic energy. The solid white line marks the time-averaged separated-region. The black rectangular box shows the domain of interest.

VORTEX CLUSTERS

There are several reasons why vortex clusters are more suitable tools for investigating turbulent flows than commonplace coherent structure. The first reason is that the coherent structure visualizations are extremely chaotic as it can be seen in figure 1. Hence, obtaining information from these excessively cluttered coherent structure domains is a problematic issue [Del Álamo et al, 2006]. Also, each vortex cluster represents single distinct structure since the vortex clusters are isolated and classified. Another reason is that the most common coherent structure identification criterion reflects the information about the iso-surface but not the structure inside. Vortex cluster visualizations, unlike coherent structures, exhibit real appearance since a single vortex cluster is generated by connecting neighbor grid points that satisfy a threshold condition. [Del Álamo et al, 2006]

The three-dimensional vortex clusters are identified as connected regions of intense discriminant of the velocity gradient, D [Chong et al, 1990] that satisfy the following condition

$$D(x, y, z) > \alpha\sqrt{\overline{D'^2(x, y)}} \tag{1}$$

Here α is the threshold constant and $\sqrt{D'^2(x,y)}$ is the standard deviation of D. Figure 3a illustrates an example of a vortex cluster that is generated by filled nodes that satisfy equation 1 in two dimensional grid points. The minimum vortex cluster volume is chosen as a 30 neighbour grid points in order to eliminate redundant small structures.

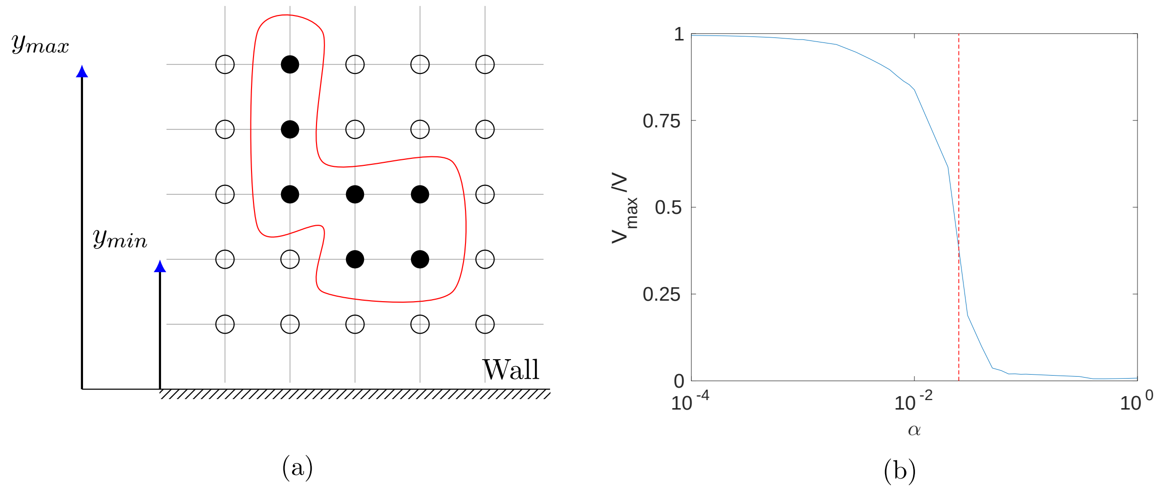

Figure 3: (a)Two dimensional example of a neighbour grid points of the vortex cluster algorithm. (b)Percolation diagram of the vortex clusters, the volume of the largest cluster normalized with total volume occupied by all clusters. Dashed-line is the threshold value $\alpha = 0.025$

In order to determine α, we performed a threshold percolation analysis as in [Del Álamo et al, 2006]. Figure 3b shows the volume ratio of the largest cluster, V_{max}, to the overall volume of the all cluster, V, inside the useful domain as a function of the threshold constant α. The volume ratio is dramatically increasing after reaching enough low threshold values. The percolation threshold is defined as α value for which the slope of the curve is maximum, which is equal to approximately 0.001. Below that specific value of α, the clusters evolve into sizeable single sponge-looking structure where $V = V_{max}$ [Del Álamo et al, 2006]. The threshold parameter for identifying structures in this study is selected as 0.025 which is a close value to the mid-point of the percolation transition. Also this threshold parameter and volume ratio, V_{max}/V, is approximately equal to the one used in a channel flow study [Del Álamo et al, 2006].
Figure 4 presents the joint probability density function (p.d.f) of the minimum y_{min} and maximum y_{max} wall distances for the vortex clusters. The vortex clusters can be grouped into two subgroups according to their wall normal position [Del Álamo et al, 2006]. The first type exists in the near wall region where $y_{min} < 0.05\delta_a$. These structures are reaching to the wall, hence they are called wall-attached clusters. The other subgroup vortex clusters are located away from the wall, $y_{min} \geq 0.05\delta_a$, and they are called wall-detached clusters. Figure 5a shows the first subgroup of vortex clusters and the figure 5b demonstrates a wall-detached vortex cluster. These structures are intrinsically turbulent and complex objects, and the two types of structures are different in terms of size, shape and spatial organisation.

Table 2: Total cluster numbers and volumes. Volume of the clusters are non dimensionalized with the average boundary layer thickness, δ_a.

	Total	**Attached**	**Detached**
Number of Clusters	2332430	491997	1840433
Total Volume of Clusters	1748.2	1397.8	350.4

Table 2 presents the total number of cluster and their total volume. The number of wall-attached and

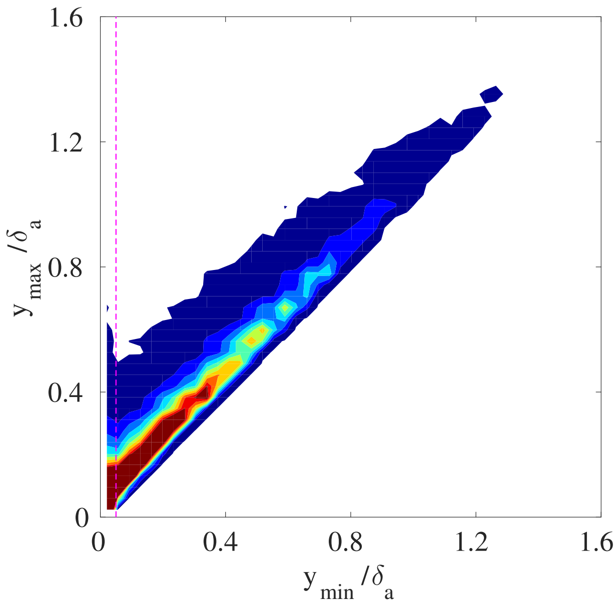

Figure 4: Joint probably density function of the vortex clusters as a function of their wall normal minimum, y_{min} and maximum distances, y_{max}. Contour levels from 0.01 to 10.

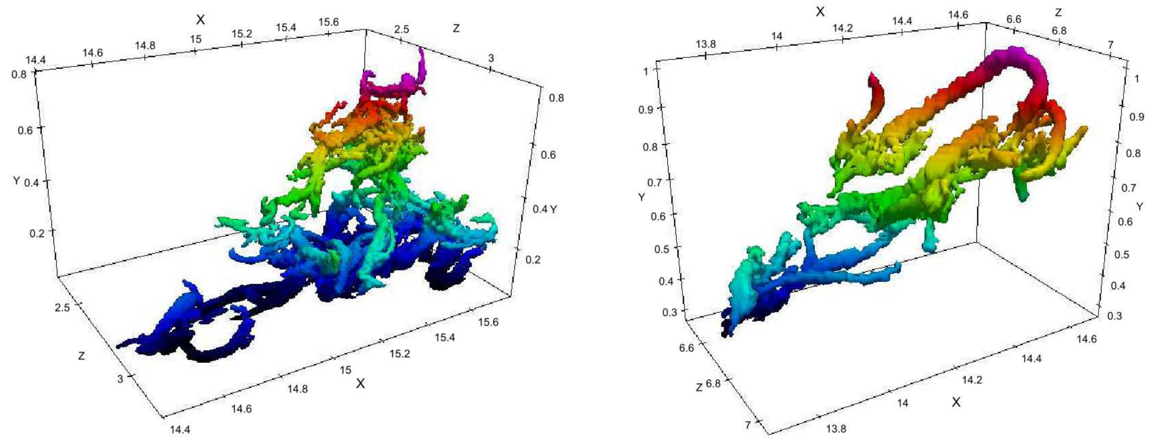

(a) Wall-attached vortex cluster

(b) Wall-detached vortex cluster

Figure 5: Representation of three dimensional vortex clusters coloured with distance from the wall; dark blue for nearest to the wall and magenta for furthest to the wall.

detached clusters are also given in table. Although almost % 80 of the clusters are detached clusters, the attached clusters occupy approximately % 80 total volume. Hence, attached clusters cannot be ignored by looking their numbers even if they are less.

RESULTS AND DISCUSSIONS

Vortex clusters dimensions are taken as a distances of parallelepiped box of vortexes. We compare the streamwise, Δ_x, wall-normal, Δ_y, and spanwise, Δ_z, box dimensions with each other and with their wall centre distances y_c.

Figure 6 depicts the vortex clusters' cubic and wall centre distances on two dimensional cluster sketch.

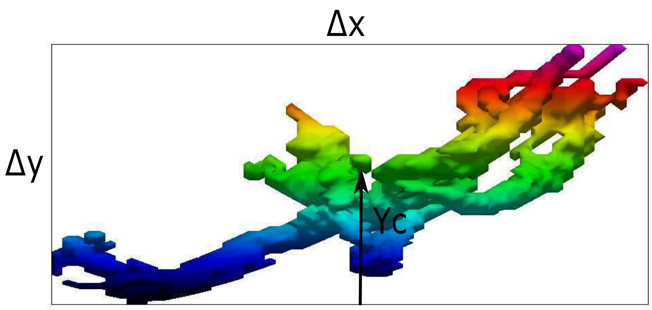

Figure 6: Two dimensional sketch of a vortex cluster. Flow is from left to right. Cluster is colored with distance to the wall

Wall-Detached Clusters

Figure 7 illustrates the joint probability density function of the logarithms of wall paralel box distances of the detached clusters and their wall distances. The joint p.d.f. that is given in the figures can be organized along as

$$5 \times \Delta x = y_c \quad 5 \times \Delta z = y_c \qquad \Delta x = \Delta y \quad \Delta z = \Delta y \tag{2}$$

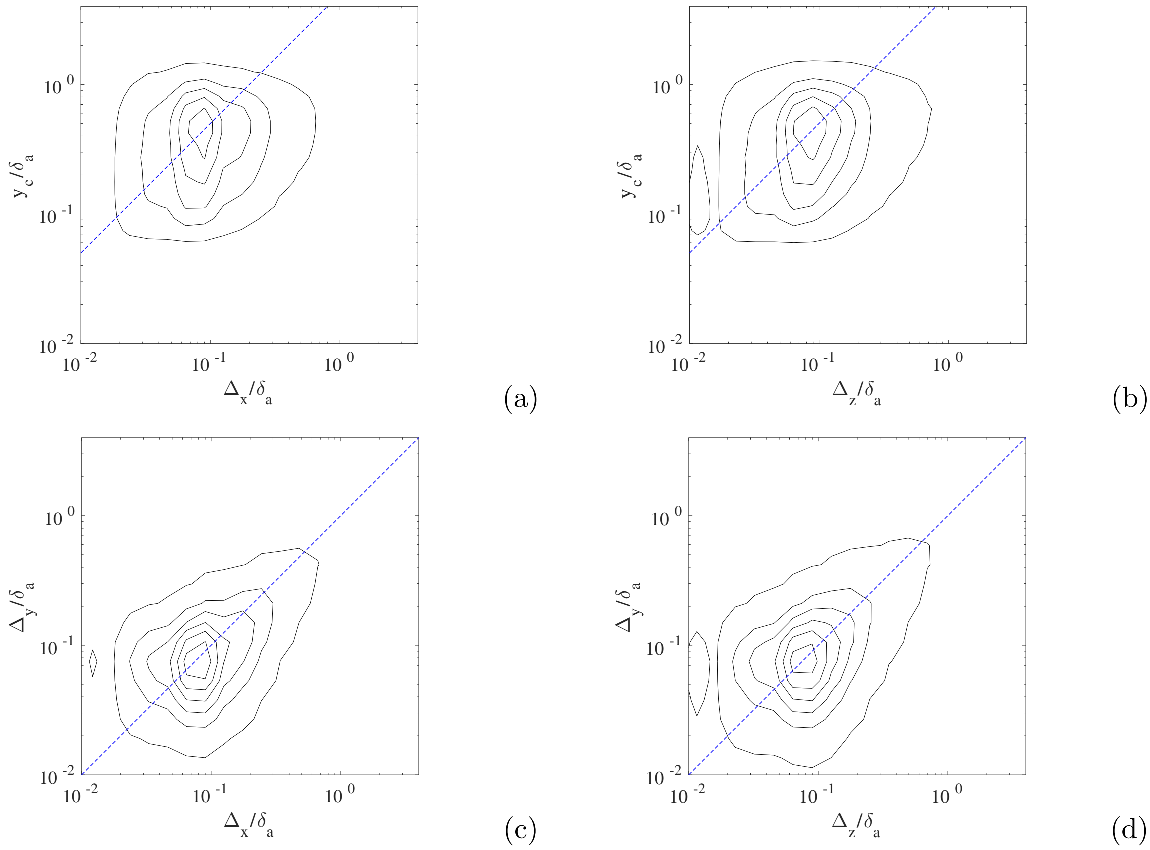

Figure 7: Joint probability density function of the parallelepiped box of the wall detached clusters and their wall distances, dashed lines are $5 \times \Delta x = y_c$, $5 \times \Delta z = y_c$, $\Delta x = \Delta y$ and $\Delta z = \Delta y$ in (a),(b),(c) and (d) respectively.

As can be seen in equation 2, the detached vortex clusters have the same box length in all three dimensions and these box lengths are proportional to their wall centre distances. This result indicates that the shape of parallelepiped box of wall detached clusters resembles to cubic boxes. Consequently, the statistical characteristic of this chaotic structures is independent of the direction of flow. As expected, this means that the detached structures show isotropic turbulence behavior in APG flow.

[Del Álamo et al, 2006] shows that detached clusters in channel flow has different parallelepiped length ratio from their wall distances. Their streamwise lengths are more than wall-normal and spanwise directions. Hence, wall-detached vortex clusters in APG flows have less elongation than channel flows.

Wall-Attached Cluster

Figure 8 illustrate the joint p.d.f of the logarithms of wall parallel box distances of the attached clusters and their wall distances. The joint p.d.f. that is given in the figures can be organized along as

$$0.7 \times \Delta x = y_c \quad \Delta z = y_c \qquad 0.7 \times \Delta x = \Delta y \quad \Delta z = \Delta y \tag{3}$$

The wall-attached clusters are significantly different from than detached ones. As can be seen in equation 3, the attached vortex clusters, unlike the detached ones, have more elongation on streamwise direction and vortex clusters dimensions are proportional to their wall centre distances. The lengths and widths of these wall-attached structures are proportional to wall normal, Δ_y, distances. Also these structures have same box lengths on wall normal and spanwise direction. Because of their large size, attached clusters have more box lengths in x direction than their wall centre distances, unlike wall-detached ones. On the other hand [Del Álamo et al, 2006] illustrate that attached clusters in channel flow have more elongation on x distances same as here in APG flows.

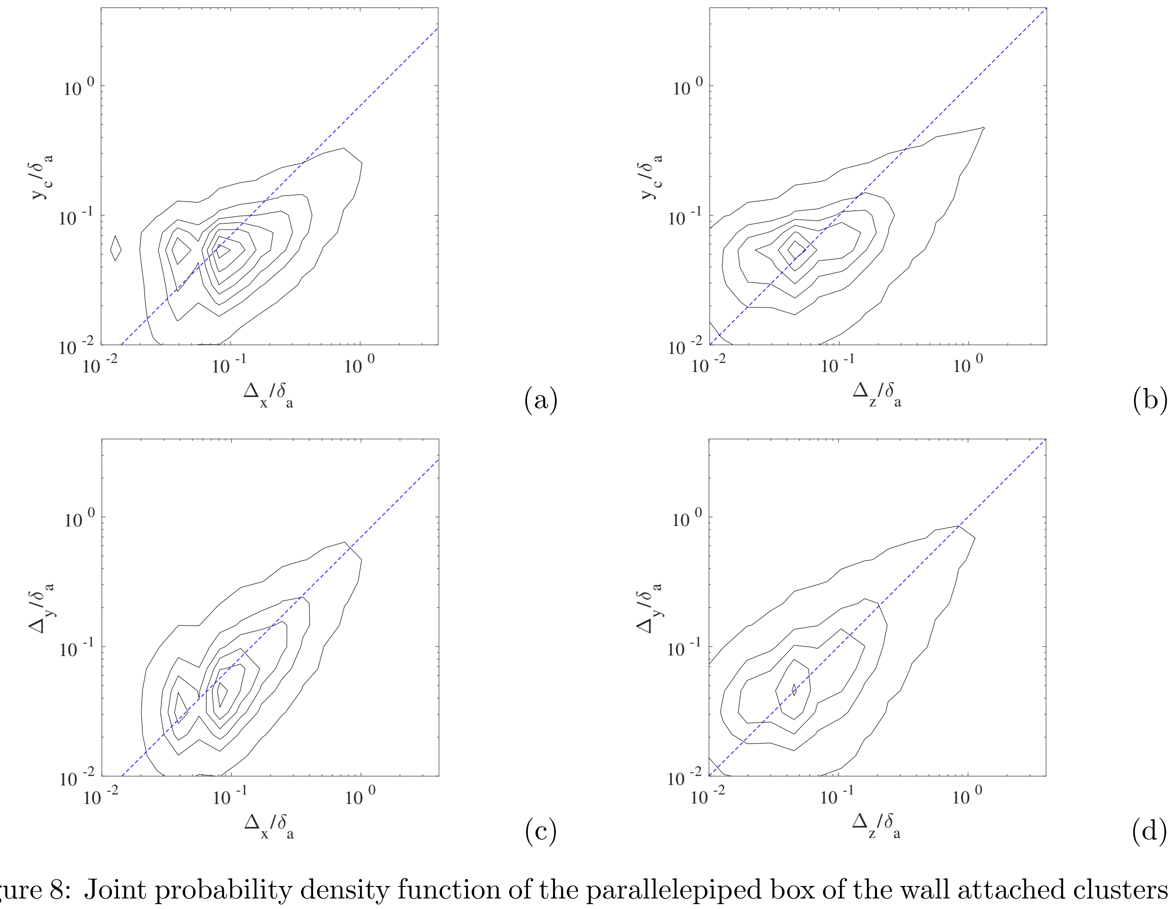

Figure 8: Joint probability density function of the parallelepiped box of the wall attached clusters and their wall distances, dashed lines are $0.7 \times \Delta x = y_c$, $\Delta z = y_c$, $0.7 \times \Delta x = \Delta y$ and $\Delta z = \Delta y$ in (a),(b),(c) and (d) respectively.

APG Effects on Clusters

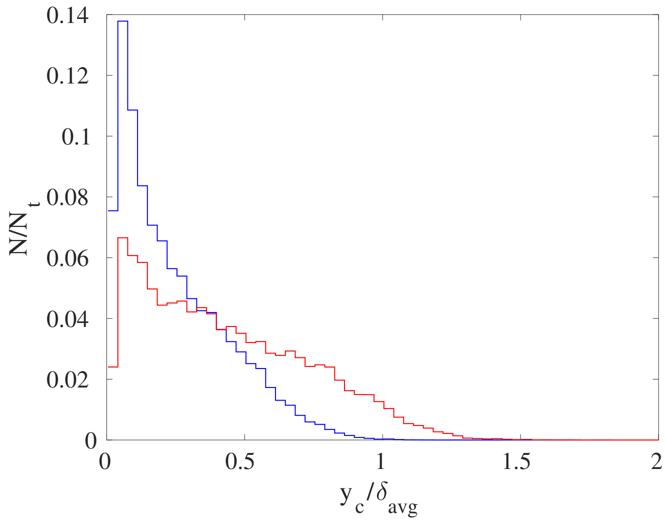

Figure 9: Probability density function of the wall centre distances. Clusters numbers are normalized with their maximum cluster number in that location. Blue line at $x/\delta_{avg} = 12$ and red line at $x/\delta_{avg} = 15$.

Figure 9 shows the APG effect on vortex distribution in the wall normal direction at two streamwise location. There is a considerable decrease in the possibility of occurrence of wall-attached clusters as the APG flow evolves in the streamwise direction. Also figure indicates that as the flow proceed in the streamwise direction with increasing APG effect, the vortexes tend to move away from the wall.

Vortex Clusters with Q Method

Vortex clusters that identified with D method had analyzed statistically. Nonetheless there is more than one vortex identification method and there are no statistically significant differences between these vortex identification methods [Chakraborty et al, 2005]. The difference between Q [Hunt et al, 1988] and D method is their power of the velocity derivatives. The D method is a sixth power of the velocity derivatives and Q is a second power of the velocity derivatives [Chakraborty et al, 2005].

[Dong et al, 2017] uses Q criterion in their vortex cluster identification and [Lozano-Durán et al, 2015] stated that higher-order quantities have tendency to be meaningless when the resolution borderline. To illustrate that the vortex cluster statistics are independent of their identification method, the same methodology used for the Q vortex cluster identification method.

Although identification method has changed, the percentage of the clusters numbers and their volume occupation has not changed. Also exactly same vortex elongation and distribution as in D method were obtained from Q method.

CONCLUSION

Statistical properties of vortex clusters in a turbulent boundary layer subjected to strong APG flow are investigated using a DNS data which mimics the flow over suction side of a low pressure turbine. Vortex clusters are identified by using two criteria of vortex identification techniques; Q criterion and D criterion.

Results show that vortex clusters are split in to two groups according to their wall normal position: wall-attached and wall-detached. The joint probability density function of the box distances of these vortex clusters indicate that the box dimensions of the wall-detached ones are independent of the direction of the flow. This behavior indicates that this type of clusters show isotropic behavior in APG flow. While attached vortex clusters shows that they have more elongation on streamwise direction

and their heights and widths are proportional to their wall normal distances.
The probability density function of the wall centre distances at two streamwise location clearly indicates that as the APG flow evolves in the streamwise direction, the vortex clusters tend to move away from the wall.
Additionally, the statistical characteristic of vortex clusters were shown to be unchanged with the vortex identification techniques.

ACKNOWLEDGMENT
We would like to thank Dr. Adrián Lozano Durán and Prof. Javier Jiménez for the processing programs for the vortex cluster analysis and Cansu Uzay for assistance in creating figure 1.

References

Aubry, N., Holmes, P., Lumley, J. L. and Stone, E. (1988). *The dynamics of coherent structures in the wall region of a turbulent boundary layer.*, Journal of Fluid Mechanics, Vol 192, p. 115-173, 1988

Chakraborty, P., Balachandar, S., and Adrian, R. J. (2005). *On the relationships between local vortex identification schemes*, Journal of Fluid Mechanics, Vol 535, p. 189-214, 2005

Chong, M., Perry, A.E. and Cantwell, B. (1990). *A general classification of three-dimensional flow fields.*, Physics of Fluids A: Fluid Dynamics (1989-1993), Vol 2, p. 765–777, 1990

Del Álamo, J. C., Jiménez, J., Zandonade, P. and Moser, R. D. (2006). *Self-similar vortex clusters in the turbulent logarithmic region*, Journal of Fluid Mechanics, Vol 561, p. 329-358, 2006

Dong, S., Lozano-Durán, A., Sekimoto, A. and Jiménez, J. (2017). *Coherent structures in statistically stationary homogeneous shear turbulence.*, Journal of Fluid Mechanics, Vol 816, p. 167-208, 2017

Gungor, A. G., Maciel, Y., Simens, M. P. and Soria, J. (2014) *Analysis of a turbulent boundary layer subjected to a strong adverse pressure gradient*, Journal of Physics: Conference Series, Vol. 506, No. 1, p. 012007, 2014

Hunt, J.C., Wray, A. and Moin, P. (1988). *Eddies, streams, and convergence zones in turbulent flows*, Center for Turbulence Research Report, p. 193-208, 1988

Hussain, A. F. (1983) *Coherent structures-reality and myth*, Physics of fluids, Vol 26, No. 10, p. 2816-2850, 1983

Lozano-Durán, A., Holznerb, M. and Jiménez, J. (2015). *Numerically accurate computation of the conditional trajectories of the topological invariants in turbulent flows.*, Journal of Computational Physics, Vol 295, p. 805-814, 2015